1	A Diagnostic Approach to Modeling Watersheds with Human Interference
2	M. Garcia <sup>1</sup> , B. Mohajer Iravanloo <sup>2</sup> , and M. Sivapalan <sup>3</sup>
3 4	<sup>1</sup> School of Sustainable Engineering and the Built Environment, Arizona State University, Tempe, AZ, USA.
5 6	<sup>2</sup> School of Sustainable Engineering and the Built Environment, Arizona State University, Tempe, AZ, USA.
7 8	<sup>3</sup> Department of Civil and Environmental Engineering, and Department of Geography and Geographic Information Science, University of Illinois at Urbana-Champaign, Urbana, IL, USA
9 10	Corresponding author: Margaret Garcia (M.Garcia@asu.edu)

#### Abstract

Most watersheds have human impacts that modify hydrological responses differently over a range of timescales. However, these impacts are not accounted for in most hydrological models. Human impacts in watersheds are diverse and case specific, unlike natural hydrologic processes. Incorporating all plausible human impacts comes at a high data acquisition and modeling cost. This raises the question, which human impacts do we need to incorporate to represent observed streamflow patterns at different timescales? To answer this question, we develop a diagnostic approach to modeling watersheds with human interference. This mixed methods approach is informed by the case history and builds on the top-down hydrological modeling approach where process complexity is incrementally added with changing timescales to identify and respond to changing dominant hydrological processes in a given watershed. Here we implement this modeling approach in the East Fork watershed in California, USA for which data on changes in water imports, withdrawals, irrigation and agriculture land cover is available from the early 1940's, making it an ideal demonstration case. In the East Fork watershed, we find that incorporation of water imports and rights are sufficient to replicate annual patterns of runoff variability, and that adding crop water demand and irrigation enables replication of monthly and daily patterns, while incorporation of groundwater pumping results in negligible improvements. To demonstrate the capabilities of the diagnostic approach in and beyond this case we conducted two computational experiments: checking for needed model structural change and exploring a counterfactual scenario of intensified agriculture. 

# 1.0 Introduction

Human activity has shaped the hydrological cycle for generations. As far back as 1864, G.P. Marsh observed that human actions can both spark and halt hydrological change. Marsh observed that clearing forests for agriculture changes the patterns of soil drainage and affects local humidity levels. Similarly, he found that clearing fallen trees and other debris from waterways stops the formation of bogs and the lateral movement of streams (Marsh, 1965). Over time our understanding of the extent of human impacts on the hydrological cycle has increased. Land cover change alone impacts infiltration, groundwater recharge, surface water flow regimes, water quality, biodiversity, and water and energy budgets (Sehot & Wal, 1992; Sivapalan, 1996; Tong & Chen, 2002; Vahmani & Hogue, 2014; Vörösmarty et al., 2010; Wissmar et al., 2004). Further, these impacts span the sub-meter, watershed, and global scales (Bhaduri et al., 2000; Reyes et al., 2015; Vörösmarty et al., 2010). In recent decades, human impacts on Earth systems, including hydrological systems, have accelerated (Steffen et al., 2015) and most watersheds now have some degree of human impacts on hydrological responses (Bosmans et al., 2017; Haddeland et al., 2014).

This increased human influence on hydrological responses intensifies the challenge of building process understanding and predicting hydrological variables of interest as human influence can amplify or dampen hydrological processes, introduce new processes, and restructure the system (Wagener et al., 2010). There is growing recognition of the need to account for human impacts in hydrological modeling. Researchers have integrated human impacts into watershed hydrological models to a range of degrees. For example, Zhang et al.

(2020) investigated the impact of a single human impact, the construction of check dams. In contrast, Zhou et al. (2018) coupled the WEP-L distributed hydrological model (Jia et al., 2006) with a social water cycle model to simulate human impacted hydrology in the Haihe River Basin, an intensively developed watershed in China. Their social water cycle model included water withdrawals and use, wastewater discharge, irrigation, leakage, and drainage. A wide range of data sets were required to build and test this model including reservoir characteristics, reservoir storage time series, agricultural land area and crop types, irrigation patterns and water use data for agriculture, industry and domestic use, in addition to hydroclimatic data sets typically required for hydrological modeling. Wendt et al. (2021) developed a stylized model which reduced data demands. They modified the lumped HBV model (Van Lanen et al., 2013) structure to incorporate regional water management activities during drought, using drought management plans to parameterize the model to a series of representative systems in the UK. In recent years, several large-scale hydrological models have been developed that incorporate water use, reservoir regulation and land cover change (Veldkamp et al., 2018; Wada et al., 2017). However, data availability remains a major hurdle to incorporating these interferences and to adding processes such as groundwater pumping and interbasin transfers in large scale hydrological models (Wada et al., 2017). Regardless of scale, the genre of models currently used to study human influence have tended to be bottom-up models within which the human impacts are prescribed with appropriate parameterizations, and then the observed flow records are used to calibrate and validate these models.

The data challenges of integrating human impacts into hydrological models raise the

54

55

56 57

58

59

60

61

62

63

64

65

66

67

68

69 70

71

72

73 74 75

76

77

78 79

80

81 82

83

84

85 86

87

88

89 90

91

92

93

94

95

96

97

98

question, which human impacts do we need to incorporate to represent observed streamflow patterns at different timescales? A particular challenge in the development of watershed models to study hydrologic change is the paucity of precise historical records of the nature and extent of human-induced land cover changes and other human interferences in the hydrologic cycle. In the absence of such records hydrologists are then forced to infer or reconstruct these changes, including human interferences, from available historical records of precipitation, streamflow and proxy variables such as population. To address this challenge, in this paper we present what we call a diagnostic approach to modeling watersheds with human interferences. The purpose of taking this approach is to build understanding of the relative impact of various human impacted processes on streamflow patterns across time scales. Our approach builds upon the top-down modeling method which incrementally develops a hydrological model of appropriate complexity while generating process understanding (Sivapalan et al., 2003). The top-down approach starts with an observed temporal pattern in the variable of interest at a chosen (time) scale, and then hypothesizes and investigates the steps or processes at a lower level that could have generated that pattern. This approach stands in contrast to the bottom-up approach which integrates small scale processes at a lower level to discover what patterns might emerge at the higher system level (Klemeš, 1983). The way that Sivapalan et al. (2003) implemented it, the top-down approach involves incrementally adding complexity to hydrological models to generate understanding of which hydrological processes are required to generate specific streamflow patterns at different timescales. There have been several applications of the top-down approach to hydrologic modeling (Farmer et al., 2003a; C Jothityangkoon et al., 2001), which have helped to not only generate parsimonious models of watershed water balances but have also generated novel

insights into process controls on observed hydrologic responses in different climate settings

(Atkinson et al., 2002; Chatchai Jothityangkoon & Sivapalan, 2009; Massmann, 2020). More complex modeling approaches have advantages in explaining a higher percentage of streamflow variation or achieving better predictive performance. However, the complexity introduced challenges to the attribution of model performance to specific processes or features. Therefore, we apply the top-down approach as our goal is to diagnose what human influenced hydrological processes are important across time scales in the context of a specific case study.

In this paper, for the first time, we extend the top-down, diagnostic approach to modeling as a vehicle to interrogate observed historical precipitation-streamflow records in human impacted watersheds to make inferences about the historical, human-induced changes to the water balance and along the way also develop a parsimonious model of the changing hydrology. The goal is not to develop a universal model of human impacted catchments but introduce and test a transferable methodology to develop site-specific models based on data inference. By incrementally adding complexity in the way we model human impacts we test which processes are important in a particular catchment across timescales of interest to hydrologists: daily, monthly and annual. We demonstrate this approach in the watershed of the East Fork of the Upper Russian River in California, USA. Human activity has shaped the hydrology in the Upper Russian River for decades through well-documented water imports, allocation of rights to withdrawal surface water, irrigation and land cover change, making it an ideal test case for this modeling study. The availability of over seven decades of data presents a unique opportunity to examine the hydrological signatures of human development. The lessons learned from this modeling case study are however applicable to other human-impacted watersheds, both in terms of methodology and in terms of fundamental insights about the effects of human interferences in the hydrologic cycle. Further, the rich case history and long period of available data make this case ideal for developing an approach and setting the groundwork for future comparative studies.

# 2.0 Materials and Methods

99 100

101

102

103

104

105

106

107

108 109

110

111

112

113

114

115

116

117

118

119

120

121

122

123

Our primary goal in this study is to develop a minimalist model of the water balance response of 124 the Upper Russian River watershed over the 1942-2013 period, a period over which there has 125 been significant human interference in the watershed hydrologic cycle. Critically, we propose a 126 mixed-methods approach to developing this model, synthesizing qualitative data from the case 127 history with time series data to craft hypotheses of the model structure. The top-down modeling 128 129 methodology in "pristine" catchments begins with descriptions of the hydroclimatic setting and assembling multi-year time series of hydroclimate data (e.g., precipitation, potential evaporation, 130 and streamflow), as seen in the work of Jothityangkoon et al. (2001) and Farmer et al. (2003). 131 Modeling of the water balance of human-impacted catchments requires, in addition to the 132 hydroclimatic data, information on the history of human interferences that may have contributed 133 to the changes in hydrology. Some of this information may be in the form of time series, while 134 other information may only be qualitative, in the form of case narratives, which may have to be 135 converted to quantitative information for modeling purposes. The putting together of a case 136 narrative thus becomes part of the methodology of model development, which is what makes it a 137 mixed-methods approach. The case study description, including the hydroclimatic setting and the 138 case narrative is presented in section 2.1. 139

Then, given the availability of a "naturalized streamflow" record over the corresponding period, we carried out the model development in two phases. In the first phase, we use the top-down methodology to develop a model of "natural" hydrology prior to human interventions. In the second phase, we then extend the baseline model developed during the first phase to add features to account for the human interventions, again using the top-down methodology. It should be noted in passing that the "naturalized" streamflow record is a product of another hydrologic model. Therefore, the modeling of naturalized streamflow is simply an intermediate methodological step, a building block, on the way to a model of observed streamflow that reflects a combination of natural and human-influenced hydrological processes. This step was forced on us because historical data under pristine conditions was not available in this catchment, or in neighboring catchments. We further test all feasible combinations of hydrological and human impacts models to ensure that the use of naturalized streamflow has not biased the final model selection. Lastly, we demonstrate the use of the diagnostic approach in two applications: testing for structural change and selecting a model under a counterfactual scenario.

# 2.1 Case Study Description: Hydroclimate and Human Impact History

The East Fork of the Upper Russian River is in the Northern California Coast Range in Mendocino County, CA with the headwaters located in Potter Valley (Fig. 1). The Northern California Coastal Range has a Mediterranean climate (Koppen-Geiger climate type Csb (Peel et al., 2007)) characterized by warm dry summers and cool wet winters with approximately 80% of the precipitation occurring between November and March (Flint et al., 2018). The region experiences Pacific storm systems, due to its proximity to the northeast Pacific (Sumargo et al., 2020). Precipitation and average annual temperature also vary between years as seen in Fig. 2A-B. Streamflow patterns in the East Fork also show both the intra- and interannual variability seen in precipitation. The average annual streamflow in the East Fork is approximately 8.83 m<sup>3</sup>/s (1167 mm/yr normalized by watershed area), with a peak annual inflow of 17.32 m<sup>3</sup>/s (2287 mm/yr) in 1983 and a minimum annual inflow of 1.75 m<sup>3</sup>/s (231 mm/yr) in 1977 (Fig. 2C). Note that we use calendar years and not water years in this study as some data sets are only available on an annual basis by calendar year. This choice is justified because snow processes are not dominant in this watershed as the precipitation record shows only 19 total days of snow in the study period, resulting in no more than 2.4% of precipitation in any water year. This is to be expected as prior studies have found that the snow line during winter storms is between 1000 m and 2000 m elevation and the highest elevation in the East Fork watershed is 1195 m, making the watershed below the snow line for most storms (Kim et al., 1998).

Historic vegetation cover in the East Fork watershed included a mixture of hardwood, conifer, oak, and chaparral (Moidu et al., 2021). Currently predominant land covers include mixed forest, chaparral, orchards, hay fields, and vineyards (Potter Valley Irrigation District, 2022; USGS, 2016). This change in vegetation is hypothesized to alter monthly patterns in streamflow. Further a shift from natural to agricultural land cover is often accompanied by the construction of drainage systems which influence runoff timing. Ditch drainage systems with fast

response times are dominant in Mendocino County. As our finest time scale is daily, we did not further consider the effects of drainage.

The basin is underlain by the Franciscan Complex, which is dominated by sandstones, shales and conglomerates (Berkland & Ray, 1972). Alluvium deposits are also present, and these are characterized by a high silt and clay content, with pockets of sand and gravel (Cardwell, 1965). Throughout the Russian River basin, headwaters remain wetted throughout the year through baseflow contributions (Grantham, 2013), and in the East Fork a water transfer from the adjacent Eel River keeps flows elevated during the summer dry season. Groundwater levels at many wells show seasonal declines in the summer, although other locations show a seasonal increase due to irrigation in excess of crop water demands (Cardwell, 1965). Potter Valley annual groundwater withdrawal in 1954 was estimated to be on the order of 2.38 mm/yr (500 ac-feet/yr) (Cardwell, 1965). No more recent estimates are available at the watershed level, but the 2010 USGS estimate of Mendocino County groundwater withdrawals yields an estimate of 5.23 mm/yr normalized over the county area (Maupin et al., 2014). This leads us to hypothesize that groundwater pumping may influence the daily distribution of streamflow through its impact on baseflow and runoff generation.

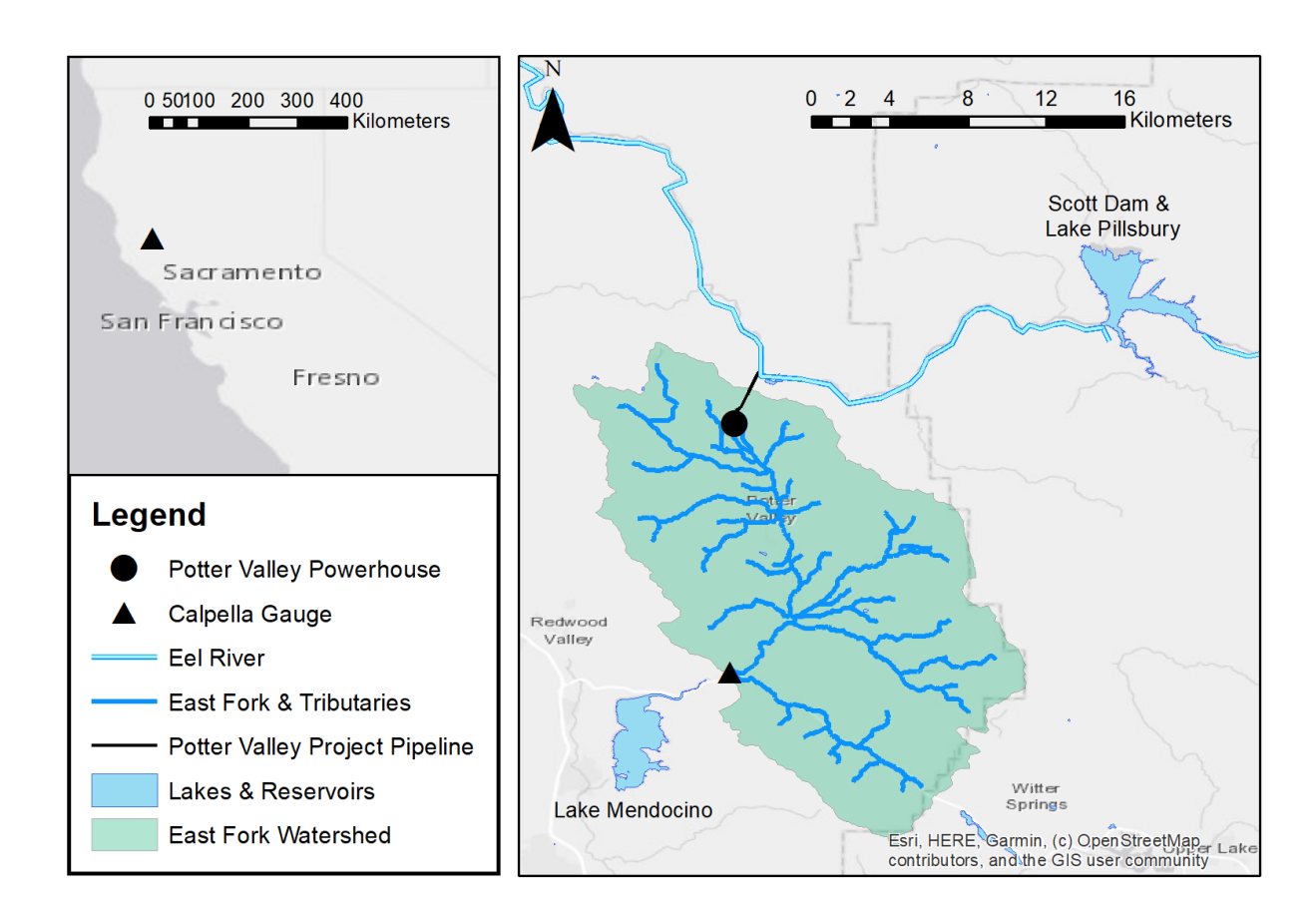


Figure 1: Location of the East Fork Watershed and the Calpella stream gauge.

The East Fork watershed above the Calpella gauge is approximately 238.7 km² (92.2 mi²) and ranges from 246 m to 1195 m above mean sea level. Lake Mendocino, formed by the Coyote Valley Dam, is located just downstream of the gauge. Lake Mendocino regulates streamflow from our study catchment including flow generated in the East Fork watershed and water diversions on the Eel River conveyed via the Potter Valley Project as a byproduct of hydropower generation. The Sonoma County Water Agency operates Lake Mendocino by collecting water for storage in the reservoir's water-supply pools when water is available for collection, and by releasing stored water to supplement natural flows as necessary (Sonoma County Water Agency, 2015). Understanding streamflow patterns in the East Fork is critical to inform long term operation of this reservoir.

The Potter Valley Project was initiated by the Eel River Power and Irrigation Company in 1900 and first generated power in 1908 (Potter Valley Irrigation District, 2022). Without upstream storage, however, the project could only generate hydropower at capacity during fall and spring; Scott Dam was constructed to store water and facilitate year-round power generation. Eel Valley residents protested the construction of Scott Dam due to concerns about damages to fish habitat and lost natural resource development opportunities locally (Langridge, 2002). In 1922, Pacific Gas & Electric Company (PG&E) acquired the system, Scott Dam was completed, and Lake Pillsbury Reservoir began to fill (Potter Valley Irrigation District, 2022). In addition to stabilizing hydropower production, Scott Dam also changed the seasonal pattern of streamflow in the East Fork, significantly increasing summer streamflow. Prior to the Potter Valley Project, the Potter Valley was dry farmed as there was little streamflow during summer months of peak crop water demand. Large scale irrigation began in 1922 and expanded in 1924 with the formation of the Potter Valley Irrigation District (Cardwell, 1965). In 1950, PG&E expanded the capacity of the Potter Valley Project transmission tunnel and entered into a contract with the Potter Valley Irrigation District to provide 1.4 m<sup>3</sup>/s (50 ft<sup>3</sup>/s) (State Water Resources Control Board Division of Water Rights, 1997). The water transferred into and withdrawn from the river is hypothesized to alter the annual water balance and therefore streamflow patterns across timescales.

The original hydroelectric power plant license issued in 1922 expired in 1972; the renewal process triggered an Environmental Impact Statement (EIS) which brought the decades old concerns about fish habitat back to the forefront (Langridge, 2002). Ultimately, the Federal Energy Regulatory Commission recommended a reduction of the water transferred from the Eel River to the East Fork. This reduction can be seen in Fig. 2D.

Fig. 2C illustrates the annual variation in streamflow observed at the Calpella gauge, normalized by watershed area (USGS, 2022). Fig. 2C also illustrates the annual variation in naturalized or unimpaired streamflow, a model product developed by the USGS that approximates streamflow in absence of human activity (Flint et al., 2015). Flint and colleagues (2013) developed the Basin Characterization Model, a gridded (270-m grid cell resolution) regional water-balance model developed for the state of California that partitions precipitation into evapotranspiration, infiltration, runoff and percolation. Applying the model Basin Characterization Model at a daily time step, Flint *et al.* (2015) used undisturbed upland

tributaries to calibrate the model for unimpaired flows in the Russian River. For model testing, they then used regression to estimate streamflow losses due to irrigation diversions and applied a conditioning method to reduce error in high and low flows and refine the calibration. Comparing the two streamflow time series gives us a window into the magnitude and patterns of human influence. From Fig. 2C we see that the magnitude of observed streamflow is higher than naturalized flow and that a decreasing trend is present only for observed streamflow. The availability of well vetted naturalized streamflow makes this case ideal for modeling the impacts of human activity on hydrological processes. In this study, we examine the trajectory of the East Fork of the Upper Russian River from 1942 (the first full year when observed streamflow is available) through to 2013 (the latest when year naturalized streamflow is available).

240241

242

243

244245

246

247

248

249

250

251

252

253

254

255

256

257

258

259

260

261

262

263

264

265

266

267

268

Variability in precipitation and temperature (Fig. 2A and B, respectively) shape both observed and naturalized streamflow. Human actions such as water imports (Fig. 2D, normalized by watershed area), expansion of agricultural and irrigated lands (Fig. 2E), and water withdrawals affect only observed streamflow. Historical data on water withdrawals is not available for this case; alternatively, we use the record of surface water rights within the watershed to approximate the upper limit of water withdrawals (California State Water Resources Control Board, 2022). Note that Fig. 2F shows water rights normalized by watershed area to facilitate comparison across variables. The State Water Resources Control Board notes that while Riparian and pre-1914 water rights holders are required to file diversion and use statements, not all water users have, leading to data gaps (State Water Resources Control Board Division of Water Rights, 1997). In addition, Grantham and Viers (2014) found that face-value water rights across California are approximately five times greater than surface water withdrawals. Therefore, we use the water rights record to approximate the maximum allowable withdrawal (irrespective of demand or physical availability of water). Water rights do not specify how water use can be distributed throughout the year. Here we assume that the usage of water rights follows the intra-annual distribution of losses (primarily due to agricultural water use) between the Capella gauge and Lake Mendocino (Sonoma County Water Agency, 2015). A full summary of data sources can be found in Table 1.

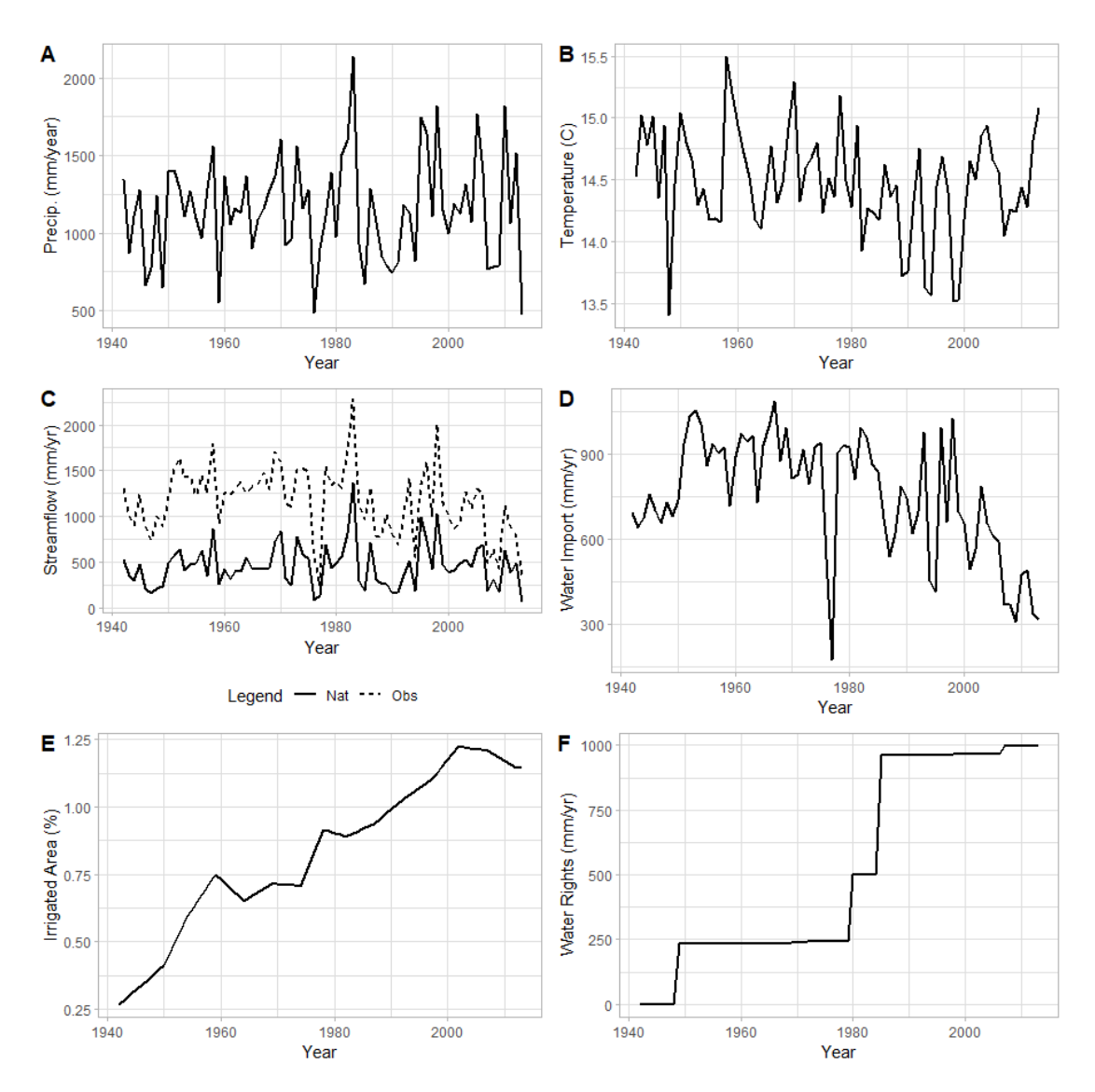


Figure 2: Annual time series of: A) precipitation, B) temperature, C) observed and naturalized streamflow, D) water Imports, E) irrigated area as a percent of total watershed area, F) water rights,

# 274 Table 1: Data sets and sources

Data Type	Source
Precipitation	Climate Data Online (NOAA, 2022a)
Temperature	Climate Data Online (NOAA, 2022b)
_	National Water Information System
Streamflow	(USGS, 2022)
Irrigated Agricultural	Census of Agriculture from 1940 to 2012
Area	(USDA, 2017)

	Electronic Water Rights Information Management System (eWRIMS)
Water Rights	(California State Water Resources Control Board, 2022)
Observed Imported Water	2011, 2012)
from the Potter Valley	
Project	Sonoma County Water Agency (2020)
Soil Types & Properties	Web Soil Survey (USDA, 2019)
Presettlement Land Cover	Wieslander Vegetation Type Mapping (Kelly et al. 2022)
	National Land Cover Database (USGS,
Current Land Cover	2016)

276

277

278

279

280

281

282

283

284 285

286

287

288

289 290

291

292 293

294

295

296 297

298

299

300

301

302

303

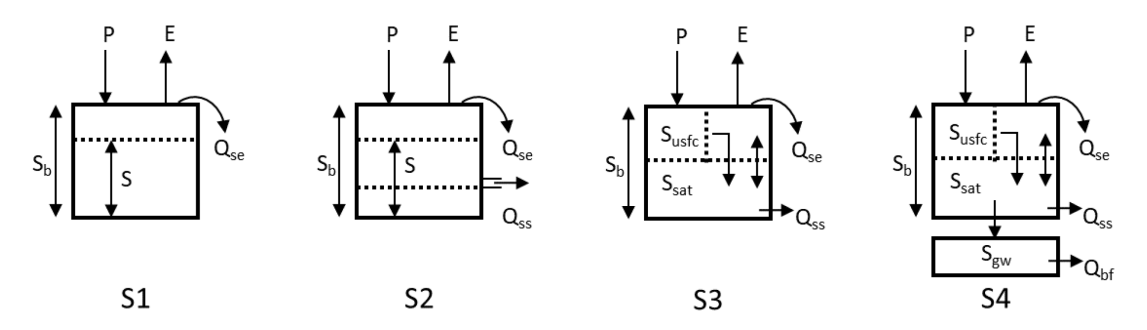
304

# 2.2 Modeling "Natural" Hydrology

We first model the natural hydrology of the Upper Russian River using the top-down approach to identify the level of hydrological process detail that must be included to reproduce annual, monthly and daily streamflow patterns. Unfortunately, we do not have streamflow and meteorological records before intensive human activity in the watershed, nor do we have an appropriate adjacent catchment for a paired catchment analysis. Therefore, we use the naturalized streamflow described above as an approximation of streamflow patterns without human influence. While naturalized streamflow is a model product not observational data, it is well vetted and used by Federal agencies (Johnson et al., 2016) and the Sonoma County Water Authority (Sonoma Water, 2021).

We use four versions of the hydrological model, developed in a series of papers by Jothityangkoon et al. (2001), Atkinson et al. (2002) and Farmer et al. (2003), starting with the simple Manabe bucket model (Manabe, 1969). More recently, these models have also been applied with minor changes by Bai et al. (2009) and Massmann (2020). Here, we apply the version of the models presented by Bai et al. (2009). All four models apply continuous moisture accounting to the chosen bucket configuration, and estimate actual evapotranspiration and forms of runoff generation, as parameterized functions of soil moisture storage. Note that potential evapotranspiration is computed using the Hamon equation and adjusted to the watershed vegetation through the selection of k<sub>v</sub> (Dingman, 2015). The models proceed from S1, the simplest, to S4, the most complex (Figure 3). Model S1 tracks moisture in a single soil volume and employs just the saturation excess runoff mechanism and accounts for evaporation and transpiration separately. Model S2 adds subsurface flow as an additional runoff mechanism, which is controlled by soil moisture in excess of a field capacity threshold. Model S3 divides the soil profile into saturated and unsaturated zones and adapts the evaporation and transpiration to separately determine fluxes from both saturated and unsaturated soil components. Lastly, model S4 adds a groundwater storage recharged via percolation and runoff generated in the form of baseflow (Bai et al., 2009). Infiltration excess, triggered by rainfall intensities greater than the infiltration capacity, is episodic. Comparing precipitation frequency estimates (NOAA, 2017) with average surface saturated hydrologic conductivity across the watershed (USDA, 2019), the

occurrence of infiltration excess with a duration of 10 minutes (26 mm/hr) would be a one-year return period event. Given the daily rainfall-runoff data, the rarity of infiltration excess in the catchment, and the challenge of diagnosing in daily data, we will only test the addition of this mechanism if model performance warrants further revisions. Snow processes are also not included in the model because of the limited snow fall as explained in Section 2.1. The full set of equations for models S1 through S4 can be found in Bai et al. (2009) and all variables and parameters are defined in the Appendix (Table A1). All models are implemented with a daily timestep and consider the East Fork watershed as a single control volume.



305 306

307

308

309 310

311

312

313

314315

316

317

318 319

320

321322

323

324

325

326 327

328

329

330

331

332

333

334

335

Figure 3: Schematic diagram of hydrological bucket models of increasing complexity (S1 simplest to S4 most complex) adapted from Farmer et al. (2003)

Most model parameters are specified directly from the data. For example, soil depth (D) and texture were extracted from 30m resolution Web Soil Survey data (USDA, 2019) and texture is used along with the relationship between texture and soil properties from Clapp and Hornberger (1978) to specify the porosity  $(\varphi)$ , field capacity  $(\theta_{fc})$  and wilting point  $(\theta_{wp})$ . Reconstructed presettlement land cover data (Kelly et al., 2005; Kelly et al., 2008) with a minimum mapping unit of 0.16 km<sup>2</sup> is used to specify the fraction of vegetation coverage (M). Spatial averages of soil and land cover parameters were used for the lumped model. For model S1 we have one calibration parameter, the interception coefficient ( $\alpha_i$ ). We add the recession coefficients for subsurface flow from saturated zone ( $\alpha_{ss}$ ) for S2. S3 has the same two calibration parameters as S2. In model S4 we add a groundwater storage volume. We further add the recession coefficient for baseflow from deep storage ( $\alpha_{bf}$ ) and the deep recharge coefficient ( $k_d$ ) for S4. The four models are fitted to the naturalized flow data in sequence. Model fit is compared using three hydrological signature plots, inter-annual streamflow variability, the monthly regime curve, and the flow duration curve, and two metrics, percent bias (Eqn. 1) and Nash Sutcliff Efficiency (NSE, Eqn. 2), computed for both real and log space streamflow (Moriasi et al., 2007). Log space metrics are used to reduce the influence of high flows on the metrics and assess model performance on average and low flows. The four metrics are used collectively to avoid a focus on matching one aspect of the hydrograph at the expense of other features (Boyle et al., 2000). Where metrics disagree, we select the model that balances performance across the metrics. Manual alternate year calibration is used to ensure that calibration and validation data sets both

contain periods with minimal and present-day levels of human activity in the watershed (Garcia

337 & Islam, 2019; Gowda et al., 2012).

338 
$$Percent \ Bias = \frac{1}{100} \left( \frac{1}{N} \sum_{i=1}^{N} Q_i^{sim} - \frac{1}{N} \sum_{i=1}^{N} Q_i^{obs} \right) = \frac{1}{100} \left( \overline{Q_{sim}} - \overline{Q_{obs}} \right)$$
 Eqn. 1

339 
$$NSE = 1 - \left[ \frac{\sum_{i=1}^{N} (Q_i^{obs} - Q_i^{sim})^2}{\sum_{i=1}^{N} (Q_i^{obs} - Q_i^{mean})^2} \right]$$
 Eqn. 2

In Eqn. 1 and Eqn. 2 above,  $Q_{obs}$  is the observed streamflow,  $Q_{sim}$  is the modeled streamflow and

N is the number of total observations.

# 2.3 Modeling Human-Impacted Hydrology

We begin our development of the human-impacted hydrological model using the best fit natural hydrological model as the foundation. However, we update the vegetation fraction (M) based on the 2016 National Land Cover Database (USGS, 2016). Then, once again, following the top-down modeling philosophy articulated by Jothityangkoon *et al.* (2001), we begin by adding fluxes and processes that are hypothesized to affect the annual water balance. Then we sequentially proceed to processes hypothesized to streamflow patterns at the monthly and finally daily time scales. This approach is also guided by our research question and interest in identifying the requisite complexity for each timescale of interest. We begin with the natural hydrology model (S4) as a zero-order model of the human-impacted hydrology which we term H0. (Subsequent models are named from H1 to HN in order of increasing complexity.) While not expected to perform well in a watershed with intensive human impacts, it serves as baseline for performance comparison.

We start the model development for human-impacted hydrology with processes hypothesized to influence annual streamflow pattern (our longest time scale) and proceed to add processes hypothesized to influence monthly and then daily streamflow patterns. From the case background and time series data (Figure 2) presented in Section 2.1, we know that there is a water transfer from the Eel River via the Potter Valley Project and a long history of water withdrawals, primarily for agricultural use. Both the transfer into the Russian River and direct withdrawals from the Russian River are likely to impact the annual water balance. However, as we have no record of withdrawals, we use water rights, a legal maximum of withdrawals, as an approximation. Therefore, our first version of the human-impacted hydrology, model H1, adds these two fluxes (Eqn. 3):

365 
$$Q = Q_{se} + Q_{ss} + Q_{bf} + T - W$$
 Eqn. 3

where T is the water transfer into the East Fork and W is water rights extraction. As these are fluxes to and from the river, there is no change to the soil moisture accounting or actual evapotranspiration, and all other equations remain the same.

After accounting for fluxes directly in and out of the river, we move to incorporate human activities affecting soil moisture dynamics, which are hypothesized to influence streamflow patterns on a monthly timescale for model H2. We first compute the irrigation demand (I) as a

- function of potential evapotranspiration (E<sub>p</sub>), precipitation (P), the percent of the watershed that
- is irrigated agriculture (A<sub>i</sub>) and the irrigation efficiency ( $\lambda_i$ ) in Eqn. 4.  $\lambda_i$  was estimated as 0.6 up
- until 1990 and 0.8 from 1990 on based on local irrigation practices and irrigation technology
- efficiency (Evans, n.d.; Lewis et al., 2008). The water for irrigation is limited to W.

$$I = \min\left(\frac{(E_p - P)A_i}{\lambda_i}, W\right)$$
 Eqn. 4

- 377 Then we modify the equations to update the unsaturated zone soil moisture (Eqn. 5) and the total
- soil moisture (Eqn. 6) to incorporate the addition of irrigation water with changes bolded:

$$\frac{dS_{us}}{dt} = P - E_i + I$$
 Eqn. 5

$$\frac{dS}{dt} = P - E + I$$
 Eqn. 6

- where  $S_{us}$  the unsaturated zone soil moisture,  $E_i$  is the interception evaporation, and S is the total
- soil moisture. We also modify Eqn. 3 to set the actual withdrawal from the river to the minimum
- of W and I.
- Lastly, we account for changes in groundwater and baseflow which may affect daily streamflow,
- particularly during low flow periods. Here we assume that irrigation demand, unmet by surface
- water rights, is pumped from groundwater (Q<sub>p</sub>) if there is sufficient groundwater in the deep
- groundwater store ( $S_{deep}$ ) and sufficient well capacity ( $Q_{p,Cap}$ ):

388 
$$Q_p = \begin{cases} \min(\min(I - W, S_{deep}), Q_{p,Cap}) & I > W \\ 0 & I \le W \end{cases}$$
 Eqn. 7

- 389 Irrigation water applied is updated to the limit of water available if insufficient water is available
- 390 to meet irrigation demand.

391 
$$I = \begin{cases} I & W + Q_p \ge I \\ W + Q_p, & W + Q_p < I \end{cases}$$
 Eqn. 8

- Lastly, the deep groundwater store is updated to account for recharge  $(r_g)$ , baseflow  $(Q_{bf})$ , and
- 393 pumping.

$$\frac{dS_{deep}}{dt} = r_g - Q_{bf} - Q_p$$
 Eqn. 9

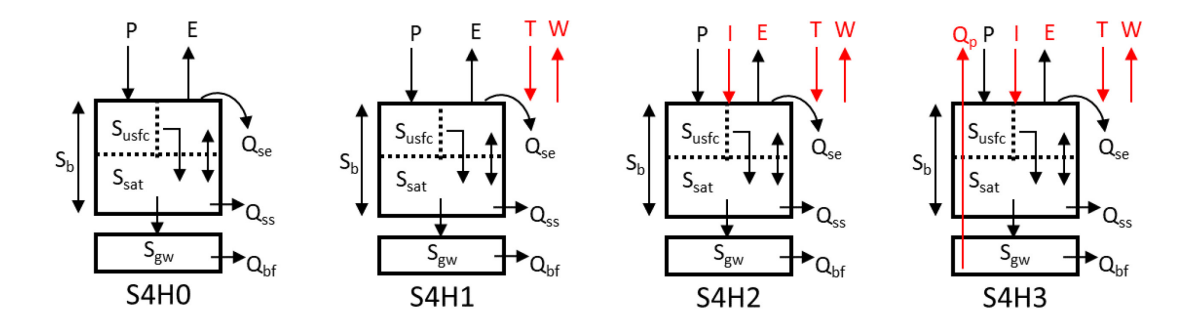


Figure 4: Schematic diagram of hydrological bucket models of increasing complexity with human directed or modified processes highlighted in red, adapted from Farmer et al. (2003)

The sequence of model development steps is presented in Figure 4, building on model S4 developed during the first phase of model development. We employ the same hydrologic signatures and metrics (percent bias and NSE) to evaluate the performance of the human-impacted hydrological model(s) and add no additional calibration parameters. Equations of model S4H3 can be found in the Appendix along with variable and parameter definitions. All other model equations can be found in the Supplemental Material (S1-S4).

# 2.4 Investigating Structural Change

A challenge of hydrological modeling in human impacted watersheds is that over time, human actions may add new processes or amplify or diminish the influence of existing processes such that model structure needs to undergo changes. The iterative diagnostic method introduced above can be applied to portions of a time series to test for model structure change. Here we identify a sharp increase in water rights in 1980 (Figure 2E). This increase is presumably in response to a general increase in irrigated agriculture and follows shortly after the record lows in annual observed flow and water imports in 1977 (Figure 2A&D). We hypothesize that this could represent a significant change in the hydrologic system, which needs to be accommodated with a change in appropriate model structure between the pre and post 1980 periods. Specifically, we hypothesize that this change could alter the relative importance of groundwater pumping (if surface water use replaced groundwater use) or change the percent of time that all irrigation demands are met, both of which have the potential to impact the model structure. To assess this, we apply the diagnostic process described in Section 2.3 separately for each period and compare the selected conceptual models.

# 2.5 Counterfactual Experiment

Counterfactuals are hypothetical scenarios of what would have occurred under conditions that differ from the historical reality (D. Lewis, 1973; Müller & Levy, 2019). Counterfactual experiments with the model can illustrate how the system would have responded if different decisions were made but exogenous factors remain as observed in the historical record. This strategy was effectively used by Srinivasan (2015) to generate key insights into human responses to droughts in the city of Chennai, India and by Penny et al. (2020) to assess the effects of the Ganges water treaty on salinity levels in the Ganges Delta. Here we examine the case of

- agricultural and irrigation intensification by scaling the historical record of expansion of irrigated
- land such that it covers 80% of the catchment by 2013 (the last year in the study period). This
- choice preserves but magnifies the existing trend and allows us to explore the hydrological
- impacts of an alternate development trajectory and the impact of model structure on streamflow
- simulation in that alternate past. Thus, the counterfactual experiment enables us to test the
- diagnostic approach under alternate conditions within a single case.

#### 3.0 Results

433

437

438

439

440

441

442 443

444

445

446

447

448 449

450

451

452

453

454

455

456

457

458 459

460

- The results are described in four parts below: modeling natural hydrology, modeling human-
- impacted hydrology, investigating structural change and applying the diagnostic approach to a
- 436 counterfactual scenario.

#### 3.1 Natural Hydrological Model Results

Figure 5 shows the hydrological signatures for naturalized streamflow and the four versions of simulated streamflow. Figure 5A illustrates the annual pattern in streamflow and shows that all four versions of the model capture most of the year-to-year variation in streamflow. Moving to monthly and seasonal patterns, we examine the regime curve in Figure 5B, which shows that model S1 tends to underestimate flows during the winter (high flow) months (December to February), while models S2 and S3 show a slight tendency to over-estimate flows during these same months. Model S4 shows the least bias during the winter months. In the spring (March through May) models S1 to S3 underestimate flows while model S4 is unbiased for March and April and biased high in May. The differences in the models are most stark at the daily timescale, as shown in the flow duration curve (Figure 5C). All models can replicate high flow days (flow exceeded on 10% of days or less) but only model S4 captures the distribution of medium to low flows. The advantages of model S4 are also clear in the model performance metrics for both the calibration and validation periods shown in Table 2. Note that the associated best fit parameters are shown in Table 3. Specifically, only model S4 shows good performance during low flows, as evidenced by the log space NSE and log space percent bias. This finding shows that surface groundwater connectivity and baseflow contributions are key to replicating the distribution of streamflow at the daily timescale. Note in passing that in previous applications of the top-down approach (e.g., Farmer et al., 2003, Atkinson et al., 2003), there was an opportunity to add further complexity to the model structure to more accurately reproduce daily streamflow in (especially) arid regions. However, we did not choose to do this here because of the good fits we already obtained with model S4. Previous work by Massman (2020) across the United States has shown that required model complexity is minimal for watersheds experiencing the Mediterranean climate, as in California.

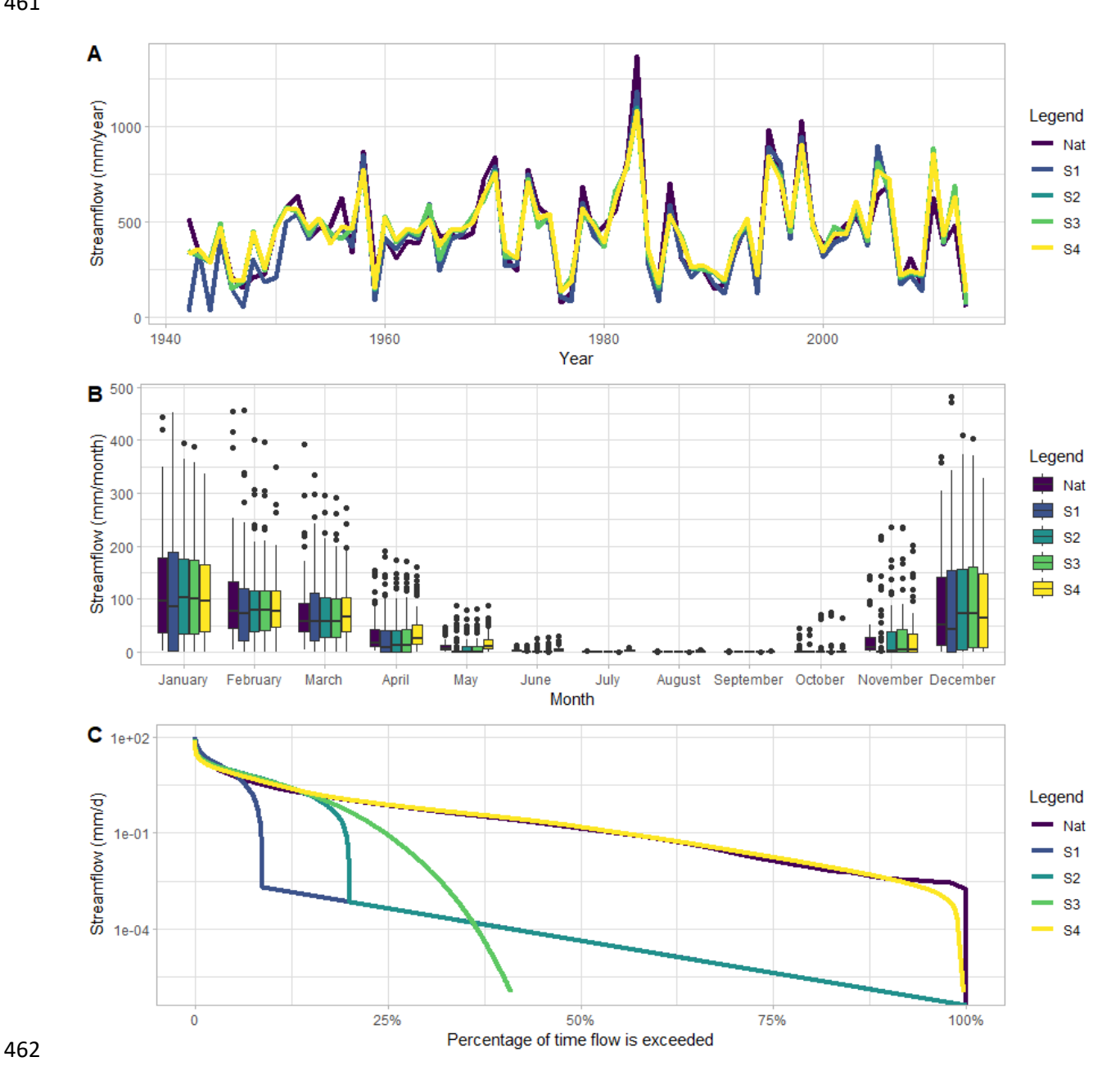


Figure 5: Hydrological signatures for naturalized streamflow and models S1-S4: A) Mean Annual Streamflow, B) Mean Monthly Streamflow, C) Flow Duration Curve

Table 2: Metrics of Model Fit for Naturalized Streamflow & Models S1-S4

Calibration				
Metric	<b>S1</b>	S2	<b>S3</b>	<b>S4</b>
NSE	0.68	0.77	0.77	0.73

Log NSE	-4.29	-1.34	-0.52	0.56
% Bias	-8.91	-1.57	-1.07	-0.42
Log % Bias	79.3	76.1	72.1	-3.71
	Va	lidation		
Metric	S1	S2	S3	<b>S4</b>
NSE	0.70	0.77	0.76	0.72
Log NSE	-4.64	-1.45	-0.63	0.51
% Bias	-6.24	1.64	2.18	3.33
Log % Bias	79.2	76.1	72.2	3.95

# 468

469

470

471

472

473 474

475

476

477

478

479

480 481

482

483

484

485

486

487

488

489

490

491

# 3.2 Human Modified Hydrological Model Results

Based on the results of modeling natural hydrology (Section 3.1), we use model S4 as a hydrological basis for adding human impacts on hydrological processes. Figure 6 illustrates the hydrological signatures for observed streamflow and the four versions of simulated streamflow. Model S4H0 (equivalent to model S4) is biased low and cannot account for interannual variability as seen in Figure 6A. The addition of water transfer and water withdrawal fluxes in S4H1 improves the model as seen in the annual timeseries (Figure 6A) and addressed the negative bias in the previous model (Table 4). However, model S4H1 cannot replicate the summer and fall (June through October) observed low flow patterns (Figure 6B). Note that streamflow simulated with S4S1 remains higher than streamflow simulated with S4H0 even as rights and irrigation increase and the transfer declines. This is because not all rights can be met due to the temporal mismatch of crop water demand and available water. The addition of irrigation driven by crop water demand in S4H2 improves the model fit at the monthly and daily timescales (Figure 6B&C). The calibration log space NSE and percent bias improve to 0.82 (0.77 for validation) and 8.00 (6.94 for validation) respectively, clearly demonstrating that model S4H2 has an improved representation of low flow processes. Lastly, model S4H3 adds groundwater pumping when surface water rights cannot meet irrigation demand. There are negligible differences between models S4H2 and S4H3 in terms of hydrological signatures (Figure 6) and metrics (Table 4). This indicates that representing groundwater pumping is not critical to matching streamflow patterns across timescales in the East Fork watershed. Note that each model version was calibrated manually and that the best fit parameters for each model versions can be found in Table 3.

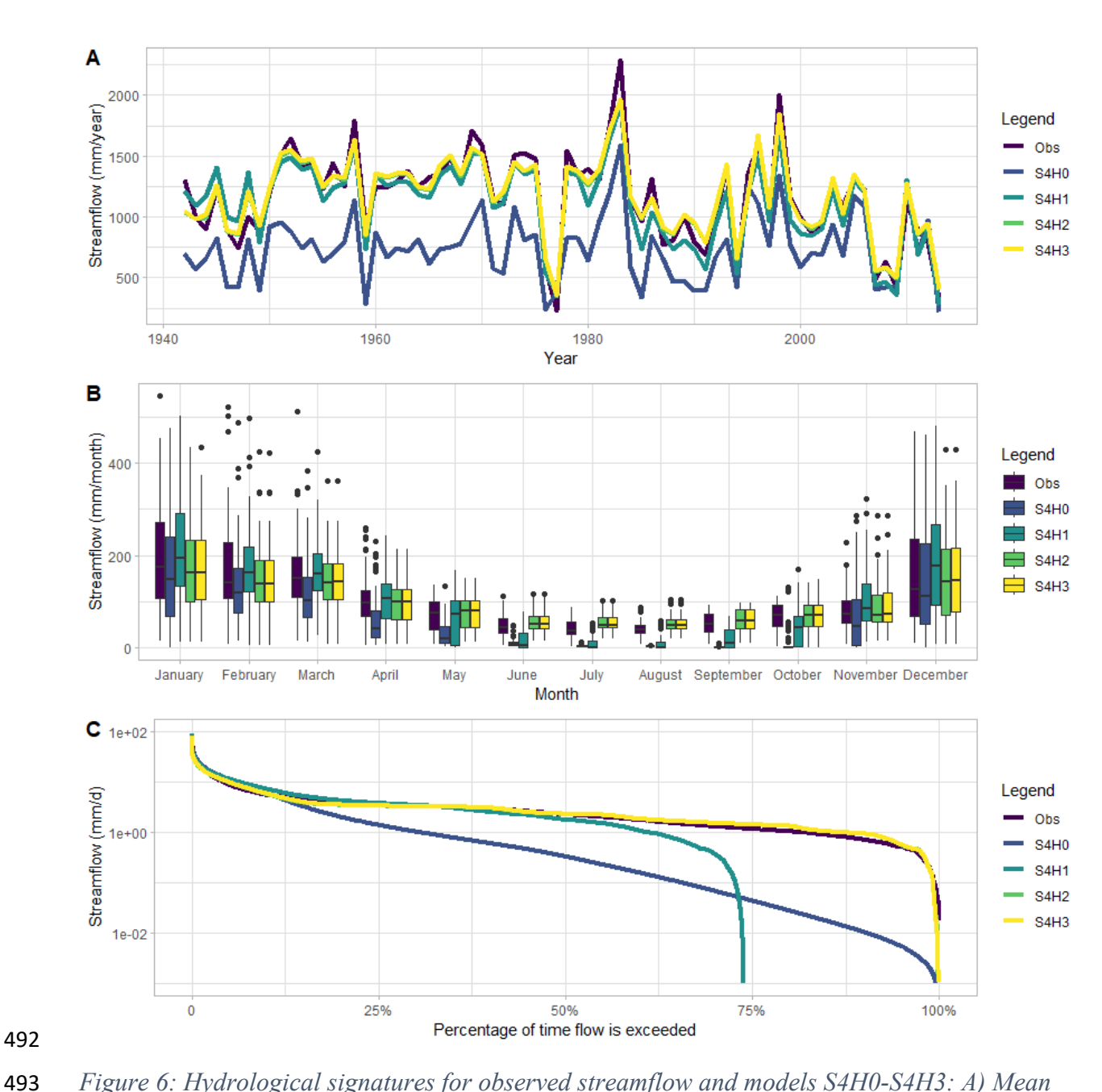


Figure 6: Hydrological signatures for observed streamflow and models S4H0-S4H3: A) Mean Annual Streamflow, B) Mean Monthly Streamflow, C) Flow Duration Curve

#### Table 3: Best Fit Parameters

Model '	Version	$\alpha_{\mathrm{ei}}$	$a_{ss}$	$a_{\mathrm{bf}}$	$k_d$
eq	S1	0.23	NA	NA	NA
Naturalized	S2	0.33	0.45	NA	NA
atur	S3	0.34	0.45	NA	NA
Ž	S4	0.34	0.45	0.025	0.15
ı D	S4H0	0.10	0.45	0.025	0.15
Human- Impacted	S4H1	0.18	0.45	0.05	0.15
Hun mps	S4H2	0.38	0.5	0.01	0.05
1 1	S4H3	0.38	0.5	0.01	0.05

Table 4: Metrics of model fit for Observed Streamflow & Models S4H0-S4H3

Calibration					
Metric	S4H0	S4H1	S4H2	S4H3	
NSE	0.69	0.77	0.73	0.73	
Log NSE	-0.49	-0.12	0.82	0.82	
% Bias	-55.6	2.18	0.64	0.51	
Log % Bias	160.2	135.7	8.00	7.65	
	Va	alidation			
Metric	S4H0	S4H1	S4H2	S4H3	
NSE	0.68	0.77	0.77	0.77	
Log NSE	-0.43	-0.13	0.77	0.74	
% Bias	-57.9	0.85	1.38	1.23	
Log % Bias	150	128.4	6.94	5.75	

As a model product, naturalized streamflow has embedded assumptions that could impact our understanding of hydrological processes presented in Section 4.1, and subsequently bias the selected model of human impacted hydrology in the East Fork watershed. To reduce the risk of such bias, we compared all feasible combinations of hydrological modules (S1-S4) and human impacts modules (H0-H3; Figure 7). Note that groundwater pumping can only be represented if groundwater storage is included in the hydrological model, therefore, only hydrological module S4 is compatible with H3. This comparison shows that while any of the selected hydrological models performs well with average to high flows as evidenced by NSE and percent bias computed in real space (Figure 7A-B), only hydrological model S4 with human impact modules H2 or H3 can adequately represent low flows as evidenced by NSE and percent bias computed in log space (Figure 7C-D). The comparison confirms that model S4H2 remains the model choice that maximizes performance across all three timescales while minimizing model complexity.

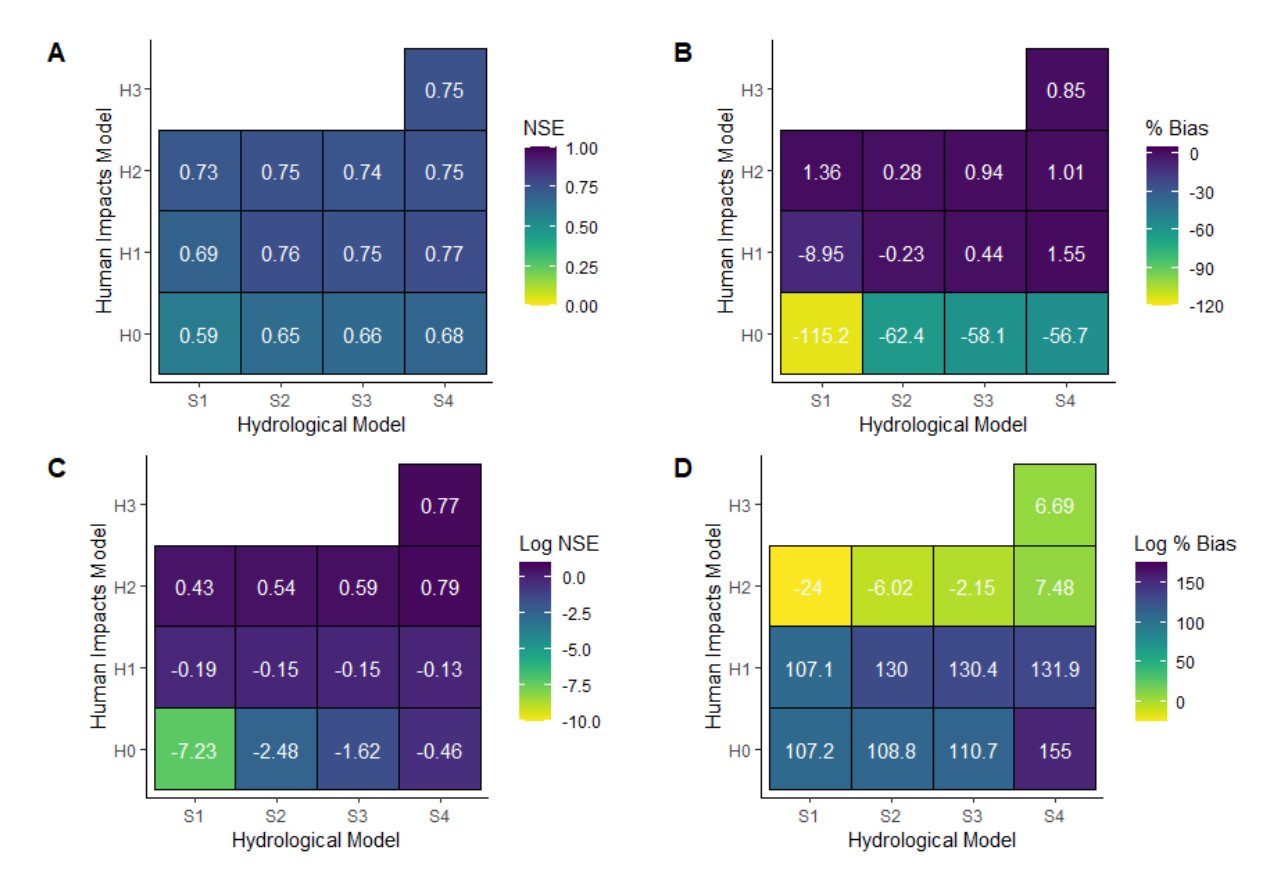


Figure 7: Comparison of all feasible combinations of hydrological models and human impacts models for: A) NSE, B) Percent Bias, C) Log space NSE, D) Log space Percent Bias.

# 3.3 Investigating Structural Change Results

While model S4H2 is a good fit for the full period, changes in water rights and irrigated area warrant investigation of structural changes over time. We apply the models for human-impacted hydrology developed above and, in this comparison, we applied the best fit parameters found in Section 4.2 and did not perform further calibration. Table 4 compares the model metrics for the period from 1942 through the end of 1979 (pre-1980) and the period from 1980 through 2013 (post-1980). Figures S5 and S6 in the Supplemental Material show the hydrological signatures for both periods. Consistent with the analysis of the full study period, models S4H0 and S4H1 do not replicate the patterns in the observed data for either pre-1980 or post-1980 periods as evidenced by low log space NSE and high log space NSE percent bias. Further, we find that in both pre- and post-1980 periods model S4H2 has improved model performance on all metrics and that introducing groundwater pumping in model S4H3 does not improve model performance. These results support the null hypothesis of no structural change in the catchment, indicating that we can proceed to apply a single model for the full period.

Table 5: Comparison of best fit models between pre- and post-1980 periods

Period	Metric	S4H0	S4H1	S4H2	S4H3
	NSE	0.68	0.79	0.76	0.76
Pre-1980	Log NSE	-0.61	0.14	0.77	0.77
re-]	% Bias	-71.8	3.83	0.18	0.17
d	Log % Bias	161.2	337.1	2.97	2.96
	NSE	0.67	0.73	0.69	0.69
Post-1980	Log NSE	-0.29	-0.45	0.82	0.82
ost-	% Bias	-40.4	-2.98	1.95	1.95
Pc	Log % Bias	146.9	114.0	13.47	13.47

# 3.4 Counterfactual Experiment

The counterfactual experiment tested the diagnostic approach's ability to detect the appropriate model structure under alternate conditions, specifically the case of agricultural and irrigation intensification. As no additional surface water is available, increased irrigation results in higher groundwater pumping. Figure 9, illustrates the differences in simulated streamflow between model structures S4H2 (irrigation but no pumping) and S4H3 (adds pumping). Compared to the historical case, there are visible differences in the simulated streamflow across annual, monthly and flow duration curve plots. Figure 9A shows that the differences between simulated streamflow from S4H2 and S4H3 grows over time which is consistent with the increase in groundwater pumping over the counterfactual period, which we attribute to reduced baseflow caused by groundwater drawdown. Figure 9C supports this interpretation as the flow duration curve shows that high and average simulated streamflow is similar across the two models while low flows are notably lower for S4H3 when groundwater pumping is incorporated. An additional computational experiment attributing streamflow change can be found in the Supplemental Material (S7).

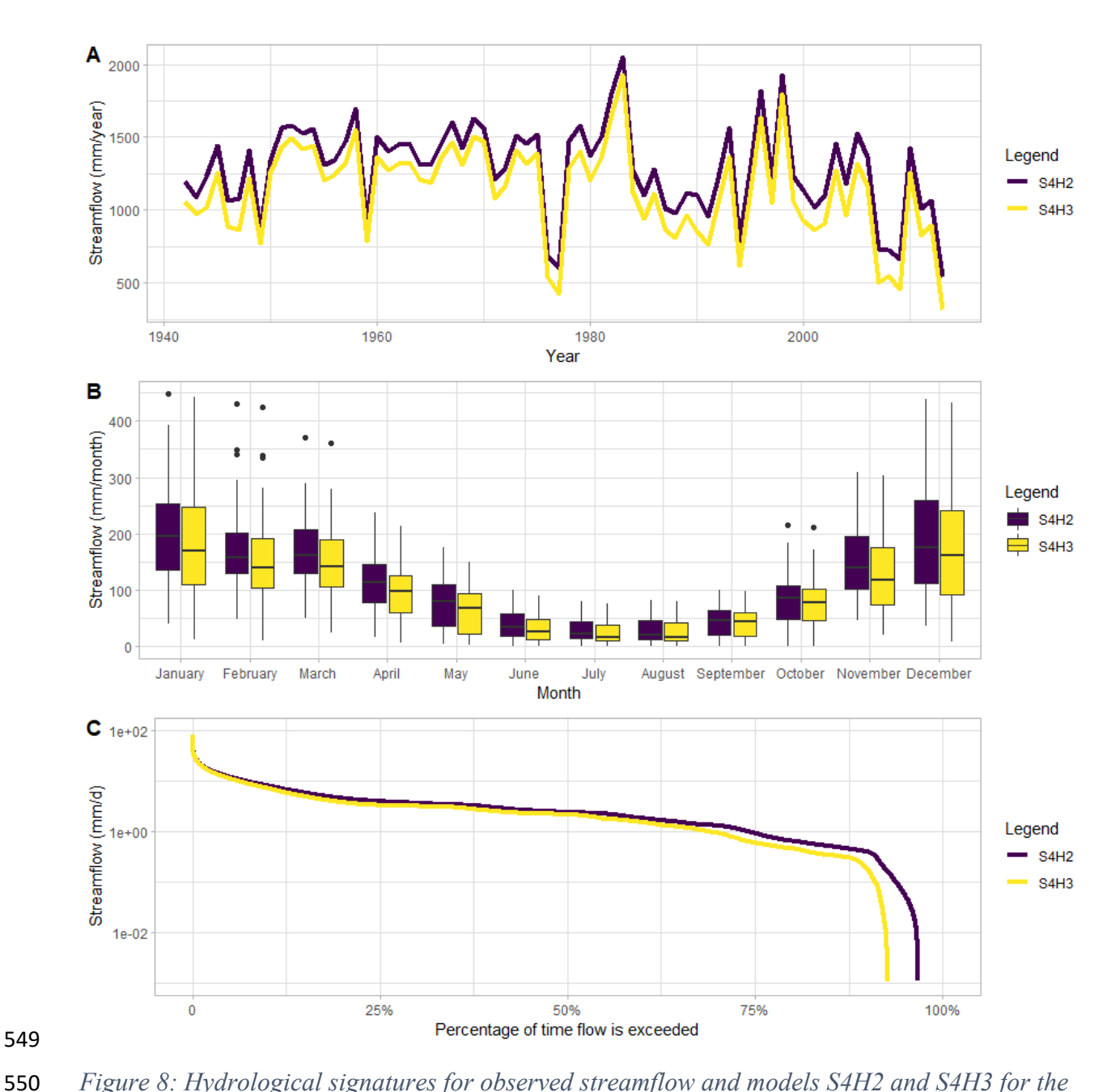


Figure 8: Hydrological signatures for observed streamflow and models S4H2 and S4H3 for the counterfactual scenario: A) Mean Annual Streamflow, B) Mean Monthly Streamflow, C) Flow **Duration Curve** 

#### 4.0 Discussion

549

551

552

553

554

555

556

557 558

559

# 4.1 Timescales and model complexity

The diagnostic approach to modeling human-impacted hydrology in the Upper Russian River has both generated case specific insights and demonstrated the potential to build generalizable knowledge of human-impacted watersheds. In the case of the East Fork of the Upper Russian River, applying the diagnostic approach to modeling natural hydrology showed that a single bucket soil moisture module with surface runoff paired with an actual evapotranspiration module

was able to capture year to year variability but not monthly or daily patterns. The addition of sub-surface runoff improved the model's ability to represent monthly patterns but only with the addition of deep groundwater storage and baseflow can the model replicate the daily streamflow distribution. This is consistent with findings in other watersheds with similar climatic aridity (Atkinson et al., 2002). Applying this diagnostic approach to the observed human-impacted streamflow demonstrated that accounting for water imports and water rights is sufficient to replicate annual streamflow patterns. However, at monthly and daily timescales, modeling irrigation based on crop water demand and irrigation efficiency is critical to replicating observed streamflow patterns. Adding groundwater pumping provides marginal improvements to the model, indicating that pumping has not impacted baseflow significantly during the study period. This is likely due to the fact that pumping has had a minimal effect on aquifer levels in this case (California Department of Water Resources, 2021), as surface-groundwater connectivity is high in the Upper Russian River (Marquez et al., 2017). The counterfactual experiment reinforces this interpretation as it illustrates that higher levels of groundwater pumping in the same catchment would result in baseflow impacts.

Collectively these findings tell us that in the East Fork watershed: 1) the annual water balance is dominated by precipitation, potential evapotranspiration, water imports and water withdrawals; 2) the monthly water balance is influenced by sub-surface runoff, crop water demand and irrigation efficiency; and 3) the daily water balance can only be explained by accounting for baseflow contributions. This is significant because different management applications emphasize different timescales. For example, water supply management typically requires an understanding of and an ability to predict monthly streamflow (U.S. Bureau of Reclamation, 2012; Wurbs, 2005). In contrast, riverine flood control operations require process understanding and predictions at the daily timescale (or shorter). Paired with this diagnostic approach, the water management application and its timescale can inform the information required to represent human impacted hydrology. Identifying the required complexity helps to decrease the data challenges of modeling human-impacts on watershed hydrology.

More broadly, the diagnostic approach presented above provides the foundation for further research to identify patterns in both human and hydrological characteristics that influence the required model complexity and best fit model structure. In comparing nine pristine catchments Atkinson *et al.* (2002) found that the aridity index of the catchment along with the timescale of interest determined the hydrological model complexity needed to replicate streamflow patterns. More recent work by Bai (2009) and Massmann (2020) confirmed these findings. Analogously, future comparative modeling studies focused on human-impacted catchments may shed light on the characteristics that influence the dominant human-impacted hydrological processes and therefore the required model structure. While further comparative work is needed to develop and test robust hypotheses, from this single case we identify relationships between catchment characteristics and direct-human impacts that may influence the model structure and complexity needed. First, we hypothesize that the strength of the surface-groundwater connection in combination with the intensity of pumping impacts model complexity. Second, we hypothesize that a larger phase shift between PET and P increases the importance of irrigation in explaining

streamflow seasonality. Future comparative work can refine and test these hypotheses as well as inform other hypotheses.

Note that while naturalized streamflow is not frequently available, the top-down approach can be applied directly to observed streamflow as demonstrated in Figure 7. However, a key obstacle to applying this approach to many catchments is that many of the required data sets are not available in a consistent form across the U.S. (or other countries) or are only available aggregated by county, which does not correspond with watershed boundaries (Maupin et al., 2018). Initiatives to assemble spatially explicit databases such as the current effort to assemble a national database of water transfers within the U.S. (Dickson et al., 2020), would greatly facilitate such comparative analyses.

# 4.2 Diagnosing changes over time

Watersheds, as with any natural system, change over time. However, human activity has accelerated the pace and expanded the scope of change, creating an additional challenge for hydrological modeling (Wagener et al., 2010). To address this challenge, in this paper we applied this diagnostic modeling approach to check for changes in the required model complexity over time. Based on a significant expansion in water rights in 1980, we separated the time series data into two periods, before and after this expansion. The diagnostic modeling approach identified the same best fit model, S4H2, for both time periods, consistent with the analysis of the full study period. This indicates that there were only quantitative and not qualitative process changes between these two periods. In contrast, the counter-factual experiment demonstrates a situation in which a model change would be needed. The experiment showed that if irrigated agriculture intensified in this watershed the magnitude of groundwater pumping could reach a level where accounting for the pumping in a hydrological model would be needed to accurately simulate streamflow. Beyond the case of the Upper Russian River, the approach can be applied to assess the need to adapt the model structure over time to account for human induced hydrological change.

#### 4.3 Limitations and Next Steps

The diagnostic approach and model developed in this study is intended to aid in diagnosis of the natural and human influenced hydrological processes that explain streamflow variability from the annual to the daily scale. Following this objective, the simplicity of the model and its iterative development is both intentional and supported by prior research (Bai et al., 2009; Farmer et al., 2003c; Chatchai Jothityangkoon & Sivapalan, 2009; Massmann, 2020). In focusing on the objective of diagnosis, the model has not been designed for prediction or decision support. However, the knowledge gained through the diagnostic analysis presented here could inform the development of improved prediction and decision support models for the East Fork watershed by targeting data collection and model refinement efforts to the most impactful variables and processes.

The diagnostic capabilities of this model could also be improved through further data collection and model refinement. The model developed in this paper is lumped and a next step is to develop a semi-distributed version of the model that breaks the East Fork watershed into sub-

catchments to better represent spatial heterogeneity in catchment properties, including land cover. Additional research could also target refinement of the representation of surface-groundwater connectivity in specific areas of the watershed and collecting additional data to assess the relationship.

#### 5.0 Conclusions

Human activity impacts hydrological responses in most watersheds globally. Hydrologists are increasingly called upon to isolate hydrologic impacts of past human actions and make predictions of future impacts under projected scenarios of human-induced changes. These human interferences and their hydrologic impacts are highly site specific, and continually evolve over time. Because of this, these impacts cannot be accounted for in most hydrological models in a generic manner. Indeed, incorporating all plausible human impacts in one model comes at a high data acquisition and modeling cost, raising the questions such as: in what way do the various human interferences impact hydrologic variability?, and, in which way should we incorporate these human impacts in hydrologic models, and at what level of detail? Given the diverse nature of human interferences, there is considerable merit to exploring this question using a data-based, top-down modeling approach. This paper represents an important first step in this direction.

This paper is aimed at developing a parsimonious hydrologic model capable of representing observed streamflow variability at multiple timescales in a highly human-impacted catchment in California. To achieve this, we developed a diagnostic approach to modeling watersheds with human interference. This approach builds on the top-down hydrological modeling approach in which process complexity is incrementally added to identify which hydrological processes are important to replicate observed streamflow patterns in a particular location and at a specific timescale. Here we incrementally added processes through which humans modify hydrology in the sub-watershed of the East Fork of the Upper Russian River in California, USA, a watershed influenced by over a century of human activity. Applying this method, we found, for example, that incorporation of just water imports and water rights can replicate annual patterns sufficiently well. However, adding crop water demand and irrigation is required to replicate monthly and daily patterns. The incorporation of groundwater pumping does not change model performance and is not needed in this case. However, in a counterfactual experiment we find that if irrigation and groundwater pumping intensified the model would require pumping to replicate patterns. Further, we apply the model to test for structural changes in the best fit model over time and to test hypotheses of the drivers of a recent decline in streamflow. We find that no changes in model structure are warranted for the 1942 to 2013 study period and that decreased water imports best explains the decline in observed streamflow.

These insights into the human-impacted hydrological responses of the Upper Russian River serve to demonstrate the potential to build process understanding of human-impacted watersheds generally, and to identify both hydrological and human systems characteristics that can indicate the level of complexity and structure of model required. What this case demonstrates is that the diagnostic approach can be used to identify the minimum level of model complexity needed for the time scale of interest. This avoids unnecessary model complexity and parameterization, focusing data collection and parameterization efforts on highly influential human activities. Over

- time, this approach to modeling can be replicated in many human-impacted catchments in the 682
- region, and eventually in other more diverse regions globally. The insights so gained can then be 683
- 684 used to develop generalized understanding of human impacts on hydrology, and more generic
- models for the prediction of the effects of human impacts on hydrologic variability. 685

#### 686 **Appendix**

- 687 Model S4H3, changes from S4 in bold
- $S_h = D\phi$ 688

$$689 f_c = \frac{\left(\theta_{fc} - \theta_{wlt}\right)}{\left(\phi - \theta_{wlt}\right)}$$

- $S_{fc} = f_c S_h$ 690
- $E_i = \alpha_{ei} P$ 691
- $S_{ust} = S_{t-1} S_{satt-1}$ 692
- $S_{usfc} = f_c(S_h S_{sat,t-1})$ 693
- $I = \frac{(E_p P)A_i}{\lambda}$ 694

695 
$$Q_{p} = \begin{cases} min(min(I - W, S_{deep}), Q_{p,Cap}) & I > W \\ 0 & I < W \end{cases}$$

695 
$$Q_{p} = \begin{cases} min \left( min \left( I - W, S_{deep} \right), Q_{p,Cap} \right) & I > W \\ 0 & I \leq W \end{cases}$$
696 
$$I = \begin{cases} I & W + Q_{p} \geq I \\ W + Q_{p}, & W + Q_{p} < I \end{cases}$$
 recompute constraining for water availability

697

698 
$$S'_{us} = S_{us,t} + P - E_i + I$$
 update based on P and E<sub>i</sub>

699 
$$r_p = \begin{cases} S'_{us} - S_{usfc}, & S'_{us} \ge S_{usfc} \\ 0, & S'_{us} < S_{usfc} \end{cases}$$

$$700 S_t = min(S_b, S'_{us} + S_{sat,t-1})$$

701 
$$S_{sat,t} = min(S_b, S_{sat,t-1} + r_p)$$

702 
$$S_{us,t} = S_t - S_{sat,t}$$
 update based on recharge to the saturated zone

703 
$$S_{usfc} = f_c(S_b - S_{sat.t})$$
 update based on current  $S_{sat}$ 

704 
$$E_{v,us} = \begin{cases} \frac{S_{us,t}}{S_t} M E_p, & S_{us,t} > S_{usfc} \\ 0, & S_{us,t} = 0 \\ \frac{S_{us,t}}{S_t} M \frac{S_{us,t}}{S_{usfc}} E_p, & S_{us,t} < S_{usfc} \end{cases}$$

705 
$$E_{bs,us} = \frac{S_{us,t}}{S_t} (1 - M) \frac{S_{us,t}}{S_b - S_t} E_p$$

$$706 E_{bs,sat} = \frac{S_{sat,t}}{S_t} M E_p$$

$$707 E_{v,sat} = \frac{S_{sat,t}}{S_t} (1 - M) E_p$$

$$708 E_{bs} = E_{bs,us} + E_{bs,sat}$$

$$709 E_v = E_{v,us} + E_{v,sat}$$

$$710 E = E_i + E_{veg} + E_{bs}$$

711 
$$S_t = S_{t-1} + P - E + I$$

712 
$$Q_{bf} = \alpha_{bf} S_{deep,t-1}$$

713 
$$r_g = k_d S_{sat}$$

$$S_{deep,t} = S_{deep,t-1} + r_g - Q_{bf} - \boldsymbol{Q_p}$$

$$715 Q_{se} = \begin{cases} S_t - S_b & S_t > S_b \\ 0 & S_t > S_b \end{cases}$$

716 
$$Q_{ss} = \alpha_{ss} S_{sat,t}$$

717 
$$Q = Q_{se} + Q_{ss} + Q_{bf} + T - W$$

718 
$$S_{sat} = S_{sat} - Q_{ss} - r_g$$
 update based on losses

719 
$$S_t = S_t - Q_{se} - Q_{se} - r_g$$
 update based on losses

721 Table A1: Model variables and parameters. Note that new parameters and variables introduced
 722 to model human-impacts are shown in bold.

Notation	Definition	Unit
D	soil depth	mm
$\theta_{\mathrm{fc}}$	field capacity	dimensionless
$ heta_{ m wlt}$	permanent wilting point	dimensionless
φ	porosity	dimensionless
$f_c$	threshold storage parameter	dimensionless
$S_b$	maximum storage of the bucket model	mm
$S_{fc}$	threshold storage	mm
P	precipitation	mm d <sup>-1</sup>
E <sub>p</sub>	potential evapotranspiration	mm d <sup>-1</sup>
Е	actual evapotranspiration	mm d <sup>-1</sup>

Ei	interception	mm d <sup>-1</sup>
$E_{v}$	vegetation transpiration	mm d <sup>-1</sup>
$E_{bs}$	bare soil evaporation	mm d <sup>-1</sup>
E <sub>v,us</sub>	transpiration from unsaturated zone	mm d <sup>-1</sup>
$E_{v,sat}$	transpiration from saturated zone	mm d <sup>-1</sup>
E <sub>bs,us</sub>	evaporation from unsaturated zone	mm d <sup>-1</sup>
E <sub>bs,sat</sub>	evaporation from saturated zone	mm d <sup>-1</sup>
$S_{sat}$	soil water storage in saturated zone	mm
$S_{us}$	soil water storage in unsaturated zone	mm
Susfc	field capacity of current unsaturated zone	mm
$S_{deep}$	soil water storage in deep store	mm
S <sub>t</sub>	total soil water storage at current time t	mm
$S_{t-1}$	soil water storage of saturated zone at last time step t-1	mm
$r_{\rm p}$	recharge to saturated zone from unsaturated zone in which water storage exceeds field capacity	mm d <sup>-1</sup>
$r_{ m g}$	recharge from upper saturated zone to deeper store	mm d <sup>-1</sup>
Q	total runoff	mm d <sup>-1</sup>
Qse	surface runoff generated by saturation excess	mm d <sup>-1</sup>
$Q_{ss}$	subsurface flow originating from saturated zone	mm d <sup>-1</sup>
Q <sub>bf</sub>	base flow originating from deep store	mm d <sup>-1</sup>
M	fraction of catchment area covered by deep rooted vegetation	dimensionless
$K_{\rm v}$	vegetation transpiration efficiency	dimensionless
$lpha_{ m ss}$	recession coefficient for subsurface flow from saturated zone store in the linear storage-outflow model	d-1
$lpha_{ m bf}$	recession coefficient for subsurface flow from deep store in the linear storage-outflow model	d-1
$k_{\rm d}$	deep recharge coefficient from the upper saturated zone to the deep store	d-1
T	water transfer into the river	mm d <sup>-1</sup>
W	maximum water withdrawal from the river	mm d <sup>-1</sup>
I	irrigation applied to irrigated agricultural land	mm d <sup>-1</sup>
Ai	percent of the catchment with irrigation	dimensionless
$\lambda_{i}$	irrigation efficiency	dimensionless
$\mathbf{Q}_{\mathbf{p}}$	pumped water from the deep store	mm d <sup>-1</sup>

724 Acknowledgements 725 All authors were supported by the Collaborative National Science Foundation grant: Cross-Scale 726 Interactions & the Design of Adaptive Reservoir Operations. Specifically, MG and BMI were 727 supported by [CMMI-1913920], and MS was supported by [CMMI-1914028]. Additionally, we 728 729 thank Dingbao Wang, Ross Woods and Christa Kelleher for their careful review and feedback of this work. 730 731 **Open Research** 732 All data can be accessed in the references cited in Table 1 or requested from the Sonoma County 733 Water Authority. Additionally, we have created a HydroShare repository (Garcia et al., 2024) 734 with model code and sharable input data and will publish it once the paper is accepted. 735 736

#### 737 References

- Atkinson, S. E., Woods, R. A., & Sivapalan, M. (2002). Climate and landscape controls on water
- balance model complexity over changing timescales. Water Resources Research, 38(12), 50-1-
- 740 50–17. https://doi.org/10.1029/2002wr001487
- Bai, Y., Wagener, T., & Reed, P. (2009). A top-down framework for watershed model evaluation
- and selection under uncertainty. *Environmental Modelling and Software*, 24(8), 901–916.
- 743 https://doi.org/10.1016/j.envsoft.2008.12.012
- Berkland, J. O., & Ray, L. A. (1972). What is Franciscan? AAPG Bulletin, 56.
- 745 https://doi.org/10.1306/819A421A-16C5-11D7-8645000102C1865D
- Bhaduri, B., Harbor, J., Engel, B., & Grove, M. (2000). Assessing watershed-scale, long-term
- 747 hydrologic impacts of land-use change using a GIS-NPS model. *Environmental Management*,
- 748 26(6), 643–658. https://doi.org/10.1007/s002670010122
- 749 Bosmans, J. H. C., Van Beek, L. P. H., Sutanudjaja, E. H., & Bierkens, M. F. P. (2017).
- 750 Hydrological impacts of global land cover change and human water use. *Hydrology and Earth*
- 751 System Sciences, 21(11), 5603–5626. https://doi.org/10.5194/hess-21-5603-2017
- Boyle, D. P., Gupta, H. V., & Sorooshian, S. (2000). Toward improved calibration of hydrologic
- models: Combining the strengths of manual and automatic methods. Water Resources Research,
- 754 36(12), 3663–3674. https://doi.org/10.1029/2000WR900207
- 755 California Department of Water Resources. (2021). Basin Prioritization Dashboard. Retrieved
- 756 February 17, 2023, from https://gis.water.ca.gov/app/bp-dashboard/final/#
- 757 California State Water Resources Control Board. (2022). Electronic Water Rights Information
- 758 Management System. Retrieved from
- 759 https://www.waterboards.ca.gov/waterrights/water issues/programs/ewrims/index.html
- 760 Cardwell, G. T. (1965). Geology and Ground Water in Russian River Valley Areas and in
- 761 Round, Laytonville and Little Lake Valleys Sonoma and Mendocino Counties, California.
- Geological Survey Water-Supply Paper 1548. Washington D.C.
- Clapp, R. B., & Hornberger, G. M. (1978). Empirical equations for some soil hydraulic
- properties. Water Resources Research, 14(4), 601–604.
- 765 https://doi.org/10.1029/WR014i004p00601
- D. N. Moriasi, J. G. Arnold, M. W. Van Liew, R. L. Bingner, R. D. Harmel, & T. L. Veith.
- 767 (2007). Model Evaluation Guidelines for Systematic Quantification of Accuracy in Watershed
- 768 Simulations. *Transactions of the ASABE*, 50(3), 885–900. https://doi.org/10.13031/2013.23153
- Dickson, K. E., Marston, L. T., & Dzombak, D. A. (2020). Editorial Perspectives: the need for a
- comprehensive, centralized database of interbasin water transfers in the United States.
- 771 Environmental Science: Water Research & Technology, 6(3), 420–422.
- 772 https://doi.org/10.1039/D0EW90005B

- Dingman, S. L. (2015). Evapotranspiration. In *Physical Hydrology* (3rd ed.). Waveland Press.
- Evans, R. G. (n.d.). Irrigation Technologies Comparisons. Retrieved October 6, 2022, from
- https://www.ars.usda.gov/ARSUserFiles/21563/Irrigation Technologies Comparisons.pdf
- Farmer, D., Sivapalan, M., & Jothityangkoon, C. (2003). Climate, soil, and vegetation controls
- upon the variability of water balance in temperate and semiarid landscapes: Downward approach
- to water balance analysis. *Water Resources Research*, 39(2), 1–21.
- 779 https://doi.org/10.1029/2001WR000328
- 780 Flint, L.E., Flint, A. L., Curtis, J. A., Delaney, C., & Mendoza, J. (2015). Provisional simulated
- vnimpaired mean daily streamflow in the Russian River and Upper Eel River Basins, California,
- value of the value of value of
- from https://ca.water.usgs.gov/projects/reg hydro/russian-river-streamflow.html
- Flint, Lorraine E., Flint, A. L., Thorne, J. H., & Boynton, R. (2013). Fine-scale hydrologic
- 785 modeling for regional landscape applications: The California Basin Characterization Model
- development and performance. *Ecological Processes*, 2(1), 1–21. https://doi.org/10.1186/2192-
- 787 1709-2-25
- Flint, Lorraine E., Flint, A. L., Mendoza, J., Kalansky, J., & Ralph, F. M. (2018). Characterizing
- drought in California: new drought indices and scenario-testing in support of resource
- 790 management. *Ecological Processes*, 7(1), 1–13. https://doi.org/10.1186/s13717-017-0112-6
- 791 Garcia, M., & Islam, S. (2019). The role of external and emergent drivers of water use change in
- 792 Las Vegas. *Urban Water Journal*, 15(9), 888–898.
- 793 https://doi.org/10.1080/1573062X.2019.1581232
- Garcia, M., Mohajer Iravanloo, B. & Sivapalan, M. (2024, June 11). Model of Human Influenced
- 795 Hydrology of the East Fork of the Russian River (CA, USA) with data.
- http://www.hydroshare.org/resource/1d1f7d9e86e049ee92ce6d0df2ebdff4: CUASI Hydroshare.
- Gowda, P. H., Mulla, D. J., Desmond, E. D., Ward, A. D., Moriasi, D. N., & Transport, P.
- 798 (2012). ADAPT: Model Use, Calibration and Validation. Transactions of the ASABE, 55(4),
- 799 1345–1352.
- Grantham, T. E. (2013). Use of Hydraulic Modelling to Assess Passage Flow Connectivity for
- 801 Salmon in Streams. *River Research and Applications*, 29(2), 250–267.
- 802 https://doi.org/10.1002/rra.1591
- Grantham, Theodore E., & Viers, J. H. (2014). 100 years of California's water rights system:
- Patterns, trends and uncertainty. *Environmental Research Letters*, 9(8).
- 805 https://doi.org/10.1088/1748-9326/9/8/084012
- Haddeland, I., Heinke, J., Biemans, H., Eisner, S., Flörke, M., Hanasaki, N., et al. (2014). Global
- water resources affected by human interventions and climate change. *Proceedings of the*
- National Academy of Sciences of the United States of America, 111(9), 3251–3256.
- 809 https://doi.org/10.1073/pnas.1222475110

- Jia, Y., Wang, H., Zhou, Z., Qiu, Y., Luo, X., Wang, J., et al. (2006). Development of the WEP-
- L distributed hydrological model and dynamic assessment of water resources in the Yellow
- 812 River basin. *Journal of Hydrology*, 331(3–4), 606–629.
- 813 https://doi.org/10.1016/j.jhydrol.2006.06.006
- Johnson, L. E., Hsu, C., Zamora, R., & Cifelli, R. (2016). Assessment and applications of
- distributed hydrologic model Russian-Napa River Basins, CA.
- 816 https://doi.org/10.7289/V5M32SS9
- Jothityangkoon, C, Sivapalan, M., & Farmer, D. L. (2001). Process controls of water balance
- variability in a large semi-arid catchment: downward approach to hydrological model
- development. *Journal of Hydrology*, 254(1–4), 174–198. https://doi.org/10.1016/S0022-
- 820 1694(01)00496-6
- Jothityangkoon, Chatchai, & Sivapalan, M. (2009). Framework for exploration of climatic and
- landscape controls on catchment water balance, with emphasis on inter-annual variability.
- 323 *Journal of Hydrology*, 371(1–4), 154–168. https://doi.org/10.1016/j.jhydrol.2009.03.030
- Kelly, M., Allen-Diaz, B., & Kobzina, N. (2005). Digitization of a historic dataset: the
- Wieslander California vegetation type mapping project. *Madroño*, 52(3), 191–201.
- Kelly, Maggi, Ueda, K., & Allen-Diaz, B. (2008). Considerations for ecological reconstruction
- of historic vegetation: Analysis of the spatial uncertainties in the California Vegetation Type
- 828 Map dataset. *Plant Ecology*, (194), 37–49.
- Kim, J., Miller, N. L., Guetter, A. K., & Georgakakos, K. P. (1998). River Flow Response to
- Precipitation and Snow Budget in California during the 1994/95 Winter. *Journal of Climate*,
- 831 11(9), 2376–2386. https://doi.org/10.1175/1520-0442(1998)011<2376:RFRTPA>2.0.CO;2
- Klemeš, V. (1983). Conceptualization and scale in hydrology. *Journal of Hydrology*, 65(1–3), 1–
- 23. https://doi.org/10.1016/0022-1694(83)90208-1
- Van Lanen, H. A. J., Wanders, N., Tallaksen, L. M., & Van Loon, A. F. (2013). Hydrological
- drought across the world: impact of climate and physical catchment structure. *Hydrology and*
- 836 Earth System Sciences, 17(5), 1715–1732. https://doi.org/10.5194/hess-17-1715-2013
- 837 Langridge, R. (2002). Changing legal regimes and the allocation of water between two California
- 838 rivers. Natural Resources Journal, 42(2), 283–330.
- 839 Lewis, D. (1973). Counterfactuals. Cambridge, MA: Harvard University Press.
- Lewis, D. J., McGourty, G., Harper, J., Elkins, R., Christian-Smith, J., Nosera, J., et al. (2008).
- 841 Irrigated Agriculture Water Needs and Management in the Mendocino County Portion of the
- Russian River Watershed. Retrieved from https://cemendocino.ucanr.edu/files/17223.pdf
- Manabe, S. (1969). Climate and the Ocean Circulation I. The Atmospheric Circulation and the
- Hydrology of the Earth's Surface. *Monthly Weather Review*, 97(11), 739–774.
- https://doi.org/10.1175/1520-0493(1969)097<0739:CATOC>2.3.CO;2

- Marquez, M. F., Sandoval-Solis, S., DeVicentis, A. J., Partida, J. P. O., Goharian, E., Britos, B.
- R., et al. (2017). Water Budget Development for SGMA Compliance, Case Study: Ukiah Valley
- 648 Groundwater Basin. Journal of Contemporary Water Research & Education, 162(1), 112–127.
- 849 https://doi.org/10.1111/j.1936-704x.2017.03263.x
- Massmann, C. (2020). Identification of factors influencing hydrologic model performance using
- a top-down approach in a large number of U.S. catchments. *Hydrological Processes*, 34(1), 4–
- 852 20. https://doi.org/10.1002/hyp.13566
- Maupin, M. A., Kenny, J. F., Hutson, S. S., Lovelace, J. K., Barber, N. L., & Linsey, K. S.
- 854 (2014). Estimated Use of Water in the United States in 2010. Retrieved from
- https://pubs.usgs.gov/circ/1405/
- Maupin, M. A., Ivahnenko, T., & Bruce, B. (2018). Estimates of water use and trends in the
- 857 Colorado River Basin, Southwestern United States, 1985–2010: U.S. Geological Survey
- 858 Scientific Investigations Report 2018.
- Moidu, H., Obedzinski, M., Carlson, S. M., & Grantham, T. E. (2021). Spatial Patterns and
- 860 Sensitivity of Intermittent Stream Drying to Climate Variability. Water Resources Research,
- 861 57(11), 1–14. https://doi.org/10.1029/2021WR030314
- Müller, M. F., & Levy, M. C. (2019). Complementary Vantage Points: Integrating Hydrology
- and Economics for Sociohydrologic Knowledge Generation. Water Resources Research, 55(4),
- 864 2549–2571. https://doi.org/10.1029/2019WR024786
- NOAA. (2017). NOAA Atlas 14 Point Precipitation Frequency Estimates: CA. Retrieved
- September 22, 2022, from https://hdsc.nws.noaa.gov/hdsc/pfds/pfds map cont.html
- NOAA. (2022). GHCND:USC00047109 at Potter Valley Powerhouse. Retrieved from
- 868 https://www.ncei.noaa.gov/maps/daily/
- Peel, M. C., Finlayson, B. L., & McMahon, T. A. (2007). Updated world map of the Köppen-
- Geiger climate classification. *Hydrology and Earth System Sciences*, 11(5), 1633–1644.
- 871 https://doi.org/10.5194/hess-11-1633-2007
- 872 Penny, G., Mondal, M. S., Biswas, S., Bolster, D., Tank, J. L., & Müller, M. F. (2020). Using
- Natural Experiments and Counterfactuals for Causal Assessment: River Salinity and the Ganges
- Water Agreement. Water Resources Research, 56(4). https://doi.org/10.1029/2019WR026166
- Potter Valley Irrigation District. (2022). History of the Potter Valley Project. Retrieved from
- 876 https://www.pottervalleywater.org/history.html
- Reyes, B., Maxwell, R. M., & Hogue, T. S. (2015). Impact of lateral flow and spatial scaling on
- the simulation of semi-arid urban land surfaces in an integrated hydrologic and land surface
- model. *Hydrological Processes*, n/a-n/a. https://doi.org/10.1002/hyp.10683
- 880 Sehot, P. P., & Wal, J. Van Der. (1992). Human impact on regional groundwater composition
- through intervention in natural flow patterns and changes in land use. *Journal of Hydrology*, 134,
- 882 297–313.

- Sivapalan, M. (1996). Catchment-scale water balance modeling to predict the effects of land use
- changes in forested catchments. *Hydrological Processes*, 10(3), 393–411.
- Sivapalan, M., Bloschl, G., Zhang, L., & Vertessy, R. (2003). Downward approach to
- hydrological prediction. *Hydrological Processes*, 17(11), 2101–2111.
- 887 https://doi.org/10.1002/hyp.1425
- 888 Sonoma County Water Agency. (2015). Lake Mendocino Water Supply Reliability Evaluation
- 889 Report. Santa Rosa, California.
- 890 Sonoma Water. (2021). 2020 Urban Water Management Plan. Santa Rosa, California.
- 891 Srinivasan, V. (2015). Reimagining the past use of counterfactual trajectories in socio-
- 892 hydrological modelling: the case of Chennai, India. Hydrology and Earth System Sciences, 19,
- 893 785–801. https://doi.org/10.5194/hess-19-785-2015
- State Water Resources Control Board Division of Water Rights. (1997). Staff Report: Russian
- 895 River Watershed.
- 896 Steffen, W., Broadgate, W., Deutsch, L., Gaffney, O., & Ludwig, C. (2015). The trajectory of the
- Anthropocene: The Great Acceleration. *The Anthropocene Review*, 2(1), 81–98.
- 898 https://doi.org/10.1177/2053019614564785
- Sumargo, E., Wilson, A. M., Martin Ralph, F., Weihs, R., White, A., Jasperse, J., et al. (2020,
- 900 October). The hydrometeorological observation network in California's Russian River watershed
- development, characteristics, and key findings from 1997 to 2019. Bulletin of the American
- 902 Meteorological Society. American Meteorological Society. https://doi.org/10.1175/BAMS-D-19-
- 903 0253.1
- Tong, S. T. Y., & Chen, W. (2002). Modeling the relationship between land use and surface
- water quality. Journal of Environmental Management, 66(4), 377–393.
- 906 https://doi.org/10.1006/jema.2002.0593
- 907 U.S. Bureau of Reclamation. (2012). Appendix G2 CRSS Modeling Assumptions. In
- 908 Colorado River Basin Water Demand and Supply Study.
- 909 USDA. (2017). California Census of Agriculture. Retrieved from
- 910 https://www.nass.usda.gov/Publications/AgCensus/2017/Full Report/Census by State/Californi
- 911 a/index.php
- 912 USDA. (2019). Web Soil Survey. Retrieved October 2, 2022, from
- 913 https://websoilsurvey.sc.egov.usda.gov/App/HomePage.htm
- 914 USGS. (2016). National Land Cover Database. Retrieved September 8, 2014, from
- 915 http://www.mrlc.gov/finddata.php
- 916 USGS. (2022). Gauge #11461500 East fork of the Russian River near Calpella, CA. Retrieved
- 917 from https://waterdata.usgs.gov/ca/nwis/uv?site no=11461500

- Vahmani, P., & Hogue, T. S. (2014). Incorporating an Urban Irrigation Module into the Noah
- 919 Land Surface Model Coupled with an Urban Canopy Model. *Journal of Hydrometeorology*,
- 920 140421133412009. https://doi.org/10.1175/JHM-D-13-0121.1
- Veldkamp, T. I. E., Zhao, F., Ward, P. J., De Moel, H., Aerts, J. C. J. H., Schmied, H. M., et al.
- 922 (2018). Human impact parameterizations in global hydrological models improve estimates of
- 923 monthly discharges and hydrological extremes: A multi-model validation study. *Environmental*
- 924 Research Letters, 13(5). https://doi.org/10.1088/1748-9326/aab96f
- Vörösmarty, C. J., McIntyre, P. B., Gessner, M. O., Dudgeon, D., Prusevich, a, Green, P., et al.
- 926 (2010). Global threats to human water security and river biodiversity. *Nature*, 467(7315), 555–
- 927 561. https://doi.org/10.1038/nature09549
- Wada, Y., Bierkens, M. F. P., De Roo, A., Dirmeyer, P. A., Famiglietti, J. S., Hanasaki, N., et al.
- 929 (2017). Human-water interface in hydrological modelling: Current status and future directions.
- 930 *Hydrology and Earth System Sciences*, 21(8), 4169–4193. https://doi.org/10.5194/hess-21-4169-
- 931 2017
- Wagener, T., Sivapalan, M., Troch, P. A., McGlynn, B. L., Harman, C. J., Gupta, H. V., et al.
- 933 (2010). The future of hydrology: An evolving science for a changing world. *Water Resources*
- 934 Research, 46(5), 1–10. https://doi.org/10.1029/2009WR008906
- Wendt, D. E., Bloomfield, J. P., Van Loon, A. F., Garcia, M., Heudorfer, B., Larsen, J., &
- Hannah, D. M. (2021). Evaluating integrated water management strategies to inform
- 937 hydrological drought mitigation. Natural Hazards and Earth System Sciences, 21(10), 3113–
- 938 3139. https://doi.org/10.5194/nhess-21-3113-2021
- Wissmar, R. C., Timm, R. K., & Logsdon, M. G. (2004). Effects of changing forest and
- 940 impervious land covers on discharge characteristics of watersheds. *Environmental Management*,
- 941 34(1), 91–98. https://doi.org/10.1007/s00267-004-0224-5
- 942 Wurbs, R. A. (2005). Texas Water Availability Modeling System. *Journal of Water Resources*
- 943 *Planning and Management*, 131(4), 270–279. https://doi.org/10.1061/(ASCE)0733-
- 944 9496(2005)131:4(270)
- 245 Zhang, Z., Liu, J., & Huang, J. (2020). Hydrologic impacts of cascade dams in a small headwater
- watershed under climate variability. *Journal of Hydrology*, 590(August), 125426.
- 947 https://doi.org/10.1016/j.jhydrol.2020.125426
- 248 Zhou, Z., Jia, Y., Qiu, Y., Liu, J., Wang, H., Xu, C.-Y., et al. (2018). Simulation of Dualistic
- 949 Hydrological Processes Affected by Intensive Human Activities Based on Distributed
- 950 Hydrological Model. *Journal of Water Resources Planning and Management*, 144(12), 1–16.
- 951 https://doi.org/10.1061/(asce)wr.1943-5452.0000990